



Journal of Advanced Research in Fluid Mechanics and Thermal Sciences

Journal homepage:
https://semarakilmu.com.my/journals/index.php/fluid_mechanics_thermal_sciences/index
ISSN: 2289-7879



Double-Diffusive Nonlinear Buoyancy Force Significance on Free Convective Chemically Reacting Fluids Flow Past Vertical Riga Surface

Toyin Wasiu Akaje^{1,*}, Michael Adesola Taiwo¹, Bakai Ishola Olajuwon¹, Musiliu Tayo Raji¹, Simeon Ayoola Akinleye¹

¹ Federal University of Agriculture, Abeokuta, Ogun State, Nigeria

ARTICLE INFO

Article history:

Received 23 November 2022
Received in revised form 18 March 2023
Accepted 25 March 2023
Available online 12 April 2023

Keywords:

Riga plate; Casson fluid; Buoyancy force; chemical reaction; Dufour and Soret number

ABSTRACT

In this research, double-diffusive nonlinear buoyancy force effects on free convective chemically reacting fluids flow past a vertical plate in a Riga surface have been addressed numerically. Cattaneo-Christov theories, viscous dissipation, thermal radiation, thermophoresis and the Soret-Dufour mechanism were modelled in this paper. Also, thermal radiative heat flux was considered based on the Rosseland approximation because the fluid is optically thin. The flow equations were represented using partial differential equations (PDEs). These sets of PDEs were transformed into ordinary differential equations by utilizing suitable similarity variables. The transformed flow equations were numerically solved by employing the spectral collocation method. The outcomes show that enhancement in the velocity and temperature are observed due to an increase in Eckert number, thermal radiation and heat generation parameters. An increase in the relaxation heat and mass flux is noticed to have effects on the concentration and temperature gradient due to the presence of Soret-Dufour mechanisms. The present outcomes were compared with previously published works and are found to be in good agreement.

1. Introduction

When analyzing the thermo-physical fluid properties, a magnetic field is a crucial factor. Until a substance from outside the body is utilized to improve heat transfer, fluids like plasma, liquid metals, and electrolytes do not have high conduction of electricity. When the fluid is extremely conductive, electromagnetic force can be used to monitor fluid flow. The Riga plate is a magnetic bar that has permanent magnets and alternating electrodes. When it comes to boosting fluid electricity, the Riga plate might act as an external limitation. To reduce the hydrodynamic resistance of an electrolyte, this form of the plate was addressed by Gailitis [1]. Iqbal *et al.*, [2] used the Keller Box scheme to determine the impact of stagnation point flow via a Riga plate, and the results verified that melting heat transfer decreases temperature distribution while the radiation parameter increases it. Rasool and Zhang [3] researched second-grade nanofluidic flow past a convectively heated vertical Riga

* Corresponding author.

E-mail address: akajewasiu@gmail.com

<https://doi.org/10.37934/arfmts.105.1.5975>

plate. The focus of Loganathan and Deepa's [4] investigation was on the electromagnetic and radiative migration of a Casson fluid past a passable Riga plate. Rehman *et al.*, [5] studied symmetry analysis on a thermally magnetized fluid flow regime with a heat source/sink. Heat transfer in the presence of nano-sized particles suspended in a magnetized rotatory flow field was examined by Rehman *et al.*, [6]. Rehman *et al.*, [7] investigated the finite element technique for the analysis of a buoyantly convective multiply connected domain as a trapezium enclosure with a heated circular obstacle. The horizontal Riga plate, which is parallel to the x-axis and the y-axis is normal to it, was taken into consideration by Nasrin *et al.*, [8] in laminar, incompressible Casson fluid flows. Loganathan and Deepa [9] investigated the Casson fluid's motion past a Riga plate using changing linear stratification and chemical reaction. The impact of heated triangular ribs on hydrodynamic forces in a rectangular domain with a heated elliptic cylinder was studied by Rehman *et al.*, [10]. Finite element examination of hydrodynamic forces in a grooved channel having two partially heated circular cylinders was investigated by Rehman *et al.*, [11]. The viscoelastic nanofluid flow through a porous Riga plate has been studied using a 3D heat transfer analysis by Loganathan *et al.*, [12]. According to the research, concentration profiles drop for both homogeneous and heterogeneous reactions that involve more melting heat parameters. Alam *et al.*, [13] used a computational approach to address transient MHD radiative fluid flow via an inclined passable plate. Eswaramoorthi *et al.*, [14] published a numerical and analytical investigation that addressed the Darcy-Forchheimer motion of Williamson fluid over a Riga plate. Akaje *et al.*, [15] used a spectral collocation approach to investigate the impact of a non-uniform heat source and melting heat on a Casson nanofluid across a Riga plate.

Due to the wide range of engineering applications, thermal radiation and viscous dissipation have attracted the attention of many researchers. Processes of heat transfer benefit greatly from thermal radiation. It is highly helpful in building sophisticated energy conversion functions at high temperatures. The study by Siegel and Howell [16] discusses thermal radiation that occurs in a system because of the working fluid and emission of hot walls. As a function of viscosity, viscous dissipation entails the conversion of kinetic energy to internal energy. On generalized Burgers fluids, Khan *et al.*, [17] investigated nonlinear radiative heat flux and melting heat transfer processes. The investigation of hydromagnetic Casson nanofluid motion that radiates and chemically reacts was the focus of research by Mondal *et al.*, [18]. The influence of convective boundary conditions and thermal radiation parameters on heat and mass transfer on Walter's B fluid over a vertical stretching sheet was presented by Akinbo and Olajuwon [19]. Abdelmalek *et al.*, [20] examined the effect of radiation, heat source/sink, Newtonian heating, Arrhenius activation energy and binary chemical reaction for heat and mass transfer analysis. Tong *et al.*, [21] studied nonlinear thermal radiation on bioconvection slip motion of Oldroyd-B nanofluid with Cattaneo-Christov theories. Al-Khaled *et al.*, [22] researched the significance of nonlinear thermal radiation on the bioconvective motion of tangent hyperbolic nanofluid with gyrotactic microorganisms. Research on time-dependent bio-nanofluid with the significance of viscous dissipation and thermal radiation while varying thermophysical properties was addressed by Irfan *et al.*, [23]. Lavanya and Ratnam [24] examined the significance of thermal radiation alongside viscous dissipation on the motion of MHD micropolar fluid in a non-Darcian porous medium. MHD convective-radiative oscillatory motion of micropolar fluid chemically reacting was examined by Pal and Biswas [25] in a passable medium. Srinivasacharya and Kumar [26] studied the significance of thermal radiation on mixed convection of a nanofluid through a non-Darcy porous medium. Radiative heat transfer of inclined magnetic field on chemically reacting fluid by varying viscosity and thermal radiation has been researched by Salawu and Dada [27].

MHD-free convection mass and heat transfer motion over an accelerated vertical plate with hall current rotation and Soret-Dufour mechanism have been addressed by Sarma and Pandit [28]. Babu

et al., [29] examined MHD free convection Cattaneo-Christov motion past three distinct geometries with Brownian motion and thermophoresis. Karimi *et al.*, [30] studied MHD nano boundary layer flows over stretchable surfaces in a porous medium by employing the approximate solution called the Legendre collocation method. The study of Animasaun and Pop [31] researched non-Newtonian Carreau fluid flow driven by Catalytic surface reactions with buoyancy and stretching at the ambient environment. Mondal *et al.*, [32] addressed MHD mixed convection mass transfer through an inclined plate with a non-uniform heat source or sink. Gireesha *et al.*, [33] explored heat and mass transfer of Oldroyd-B nanofluid past a stretching sheet with nonlinear convective and uniform heat source/sink.

Most of the aforementioned previous works concentrated on the free convective flow of linear buoyancy force. None of the fluid considered the fluid flow in a stretching porous Riga plate with Cattaneo-Christov theories. Hence, to the very best of our knowledge, no studies have reported double-diffusive nonlinear buoyancy force effects on free convective chemically reacting fluids flow past a porous vertical plate in a Riga surface. Keeping this in mind, this study elucidates the double-diffusive flow of chemically reacting fluid with the significance of thermophysical properties. This study on double-diffusive flow in the presence of thermal radiation, and viscous dissipation in a Riga surface finds applications in thermal engineering, industrial engineering and most industries that produce a polymer. Due to these engineering applications, the present analysis becomes very useful to scientists and engineers.

2. Mathematical Analysis

A two-dimensional, laminar, incompressible boundary layer flow of a chemically fluid flow through a Riga plate is considered in this study with the presence of thermophoresis and Cattaneo-Christov heat flux. The temperature (T_w) and concentration (C_w) at the wall are kept constant. Soret-Dufour mechanisms are considered because level of species concentration is assumed to be large. Figure 1 presents the physical diagram of the fluid problem. The Boussinesq and boundary layer approximation is valid. The rheological equation for the needed fluid model Akaje and Olajuwon [34]:

$$\tau_{ij} = 2e_{ij} \left(\mu_b + \frac{P_y}{\sqrt{2\pi}} \right) \quad \text{when } \pi > \pi_c \quad (1)$$

$$\tau_{ij} = 2e_{ij} \left(\mu_b + \frac{P_y}{\sqrt{2\pi_c}} \right) \quad \text{when } \pi < \pi_c \quad (2)$$

where

$\pi = e_{ij}, e_{ij}: (i, j)$ – component of deformation rate

π : product based on the non – Newtonian fluid

π_c : critical value of this product

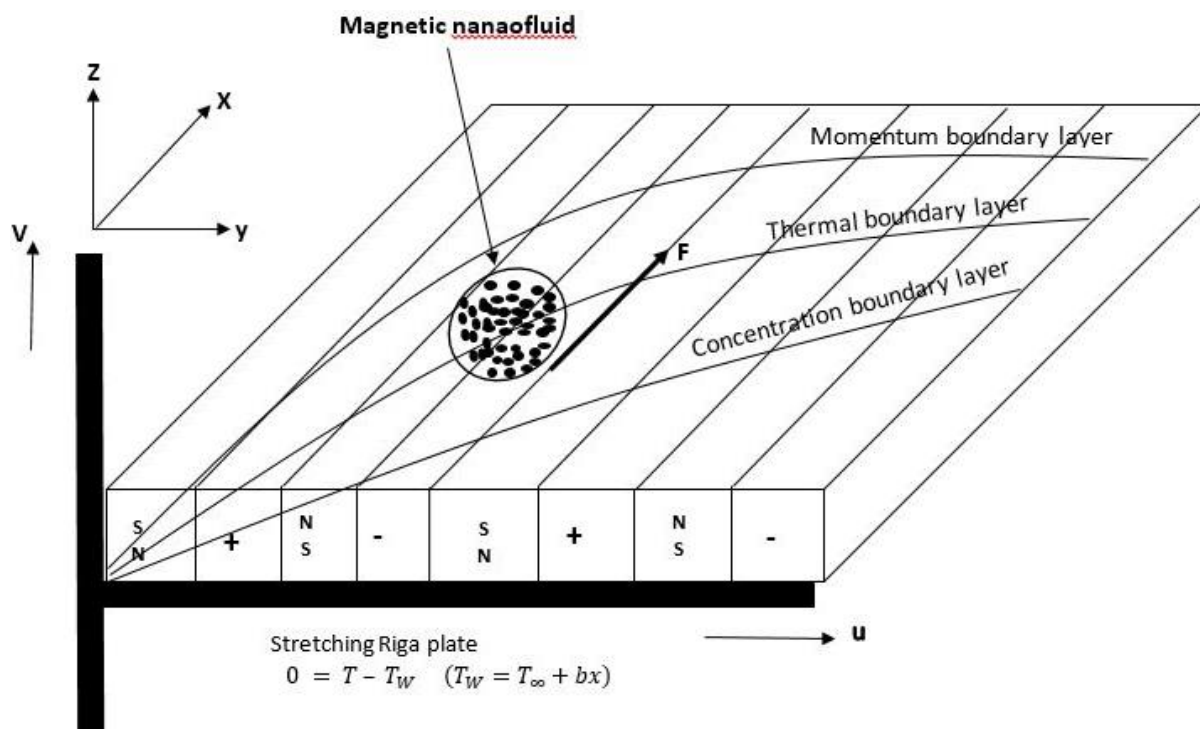


Fig. 1. Flow Geometry

The heat flux on the fluid motion is based on the utilization of Rosseland approximation as explored in Akaje and Olajuwon [34]

$$q_r = -\frac{4\sigma_s}{3k_e} \frac{\partial T^4}{\partial y} \quad (3)$$

Where Stefan-Boltzman constant= σ_s , mean absorption coefficient= k_e . It is summarized that the differences between temperature in the fluid motion are small and T^4 could be written in a linear function by simplifying T^4 about T_∞ by employing Taylor series and forgone terms of higher order to give

$$T^4 \cong 4T_\infty^3 T - 3T_\infty^4 \quad (4)$$

substituting (3) into (4), the heat flux term in the energy equation becomes

$$-\frac{\partial q_r}{\partial y} = \frac{16\sigma_s T_\infty^3}{3k_e} \frac{\partial^2 T}{\partial y^2} \quad (5)$$

Based on the exploration of Idowu and Falodun [35], V_T in concentration equation is given as

$$V_T = -k\nu \frac{\nabla T}{T_{ref}} = -\frac{k\nu}{T_{ref}} \frac{\partial T}{\partial y} \quad (6)$$

where k denotes the thermophoretic coefficient given as

$$k = \frac{2C_s \left(\frac{\lambda_g}{\lambda_p} + C_t K_n \right) \left[1 + K_n \left(C_1 + C_2 e^{-\frac{C_3}{K_n}} \right) \right]}{(1 + 3C_m K_n) \left(1 + 2\frac{\lambda_g}{\lambda_p} + 2C_t K_n \right)} \quad (7)$$

$C_1, C_2, C_3, C_m, C_s, C_t$ are constants, λ_g and λ_p denote fluid thermal conductivities and diffused particles, K_n denote the Knudsen number.

Based on all the assumptions above, the equations that govern the present model are:

$$\frac{\partial u}{\partial x} + \frac{\partial v}{\partial y} = 0 \quad (8)$$

$$\rho \left(u \frac{\partial u}{\partial x} + v \frac{\partial u}{\partial y} \right) = \mu \left(1 + \frac{1}{\beta} \right) \frac{\partial^2 u}{\partial y^2} + g\rho[\beta_1(T - T_\infty) + \beta_2(T - T_\infty)^2] + g\rho[\beta_3(C - C_\infty) + \beta_4(C - C_\infty)^2] + \frac{\pi J_0 M_0}{8\rho n_f} \exp\left(-\frac{\pi}{r_0} y\right) \quad (9)$$

$$u \frac{\partial T}{\partial x} + v \frac{\partial T}{\partial y} = \alpha_1 \frac{\partial^2 T}{\partial y^2} + \frac{Dk_T}{c_s c_p} \frac{\partial^2 C}{\partial y^2} + \frac{\mu}{\rho c_p} \left(1 + \frac{1}{\beta} \right) \left(\frac{\partial u}{\partial y} \right)^2 - \frac{1}{\rho c_p} \frac{\partial q_r}{\partial y} + \frac{Q}{\rho c_p} (T - T_\infty) - \beta_5 \left[u \frac{\partial u}{\partial x} \frac{\partial T}{\partial x} + v \frac{\partial v}{\partial y} \frac{\partial T}{\partial y} + u \frac{\partial v}{\partial x} \frac{\partial T}{\partial x} + v^2 \frac{\partial^2 T}{\partial y^2} + v \frac{\partial u}{\partial y} \frac{\partial T}{\partial x} + 2uv \frac{\partial^2 T}{\partial y \partial x} + u^2 \frac{\partial^2 T}{\partial x^2} \right] + \tau \left[D_B \left(\frac{\partial C}{\partial y} \right) \left(\frac{\partial T}{\partial y} \right) + \frac{D_T}{T_\infty} \left(\frac{\partial T}{\partial y} \right)^2 \right] \quad (10)$$

$$u \frac{\partial C}{\partial x} + v \frac{\partial C}{\partial y} = D \frac{\partial^2 C}{\partial y^2} + \frac{D_T}{T_\infty} \frac{\partial^2 T}{\partial y^2} + \frac{Dk_T}{T_m} \frac{\partial^2 T}{\partial y^2} - K'(C - C_\infty) - \frac{\partial(V_T C)}{\partial y} \quad (11)$$

Subject to:

$$u = U_w(x) = Bx, \quad v = -v(x), \quad T = T_w, \quad C = C_w, \quad \text{at } y = 0 \quad (12)$$

$$u \rightarrow 0, \quad T \rightarrow T_\infty, \quad C \rightarrow C_\infty, \quad \text{as } y \rightarrow \infty \quad (13)$$

u and v represents the relations $u = \frac{\partial \psi}{\partial y}$ and $v = -\frac{\partial \psi}{\partial x}$. This definition of u and v , the free stream is $\psi(x, y)$. It automatically satisfies the continuity equation. The following variables are utilized on the model Akinbo and Olajuwon [19]:

$$\eta = \left(\frac{B}{\nu} \right)^{\frac{1}{2}} y, \quad \psi = (\nu B)^{\frac{1}{2}} x f(\eta), \quad \theta(\eta) = (T - T_\infty)(T_w - T_\infty)^{-1}, \quad \phi(\eta) = (C - C_\infty)(C_w - C_\infty)^{-1} \quad (14)$$

The wall temperature (T_w) and concentration (C_w) and ambient temperature T_∞ and concentration C_∞ is given as follows:

$$T_w = T_0 + m_1 x, \quad C_w = C_0 + m_3 x, \quad T_\infty = T_0 + m_2 x, \quad C_\infty = C_0 + m_4 x \quad (15)$$

Employing the above similarity variables on the equations of motion (8) to (11) subject to (12) and (13) to obtain the following coupled ODE:

$$\left(1 + \frac{1}{\beta} \right) f'''' + ff'' - (f')^2 + \lambda_a \theta^2 + \lambda_b \phi^2 + Gr\theta + Gm\phi + M \exp(-\epsilon \eta) = 0 \quad (16)$$

$$\left(1 + \frac{4}{3} R \right) \theta'' + Prf\theta' + PrDo\phi'' + PrEc(f'')^2 + Nb\phi'\theta' + Nt(\theta')^2 + PrHe\theta - \alpha_1 (ff'\theta' + ff\theta'') = 0 \quad (17)$$

$$\phi'' + Scf\phi' - ScCr\phi + \frac{ScNt}{LnNb} \theta'' + \tau[\phi\theta'' + \theta'\phi'] = 0 \quad (18)$$

subject to

$$f'(\eta) = 1, f(\eta) = S_w, \theta(\eta) = (-St + 1), \phi(\eta) = (-St + 1), \text{ at } \eta = 0 \quad (19)$$

$$\theta(\eta) \rightarrow 0, f'(\eta) \rightarrow 0, \phi(\eta) \rightarrow 0, \text{ as } \eta \rightarrow \infty \quad (20)$$

$$\lambda_a = \frac{g\beta_2(T_w - T_\infty)^2}{B^2x}, \lambda_b = \frac{g\beta_4(C_w - C_\infty)^2}{B^2x}, Gr = \frac{g\beta_1(T_w - T_\infty)}{B^2x}, Gm = \frac{g\beta_2(C_w - C_\infty)}{B^2x}, M = \frac{\pi J_0 M_0}{8\rho_j x a^2}, Po = \frac{K_p B}{\mu}, ,$$

$$Pr = \frac{\nu}{\alpha}, R = \frac{4\sigma_s T_\infty^2}{Ke}, Do = \frac{Dk_T(C_w - C_\infty)}{\nu c_s c_p (T_w - T_\infty)}, Ec = \frac{(Bx)^2}{c_p (T_w - T_\infty)}, He = \frac{Q}{\rho c_p B}, Sc = \frac{\nu}{D}, Cr = \frac{K_1}{B}, So =$$

$$\frac{Dk_T(T_w - T_\infty)}{\nu T_m (C_w - C_\infty)}, \tau = \frac{K}{T_{ref}}, Nb = \frac{\tau D (C_w - C_\infty)}{\nu}, Nt = \frac{\tau D T (T_w - T_\infty)}{T_\infty \nu}, \alpha_1 = \beta_5 B$$

where the flow parameters as defined are nonlinear thermal Grashof number (λ_a), nonlinear mass Grashof number (λ_b), linear convective parameter for temperature (Gr), linear convective parameter for concentration (Gm), modified Hartman number (M), permeability term (Po), Prandtl number (Pr), radiation term (R), Dufour number (Do), Eckert number (Ec), heat generation term (He), Schmidt number (Sc), chemical reaction term (Cr), Soret number (So), Modified nanofluids thermophoresis parameter (τ), Brownian motion parameter (Nb), thermophoresis parameter (Nt), and thermal relaxation time (α_1).

The practical curiosity of engineering is local skin friction coefficient (C_f), Sherwood number (Sh) and Nusselt number (Nu). They are given in this study as follows

$$C_f = \frac{\tau_w}{\rho \nu u^2} \quad \text{where } \tau_w = \left[\left(\mu_B + \frac{P_y}{\sqrt{2\pi}} \right) \right] \frac{\partial u}{\partial y} \Big|_{y=0}$$

$$Nu = \frac{q_w}{\frac{\alpha_1}{\nu} (T_w - T_\infty)} = \theta'(0) \quad \text{where } q_w = K \left(\frac{\partial T}{\partial y} \right)_{y=0} = \frac{\alpha_1}{\nu} (T_w - T_\infty) \theta'(0)$$

$$Sh = \frac{m_w}{\frac{D}{\nu} (C_w - C_\infty)} = \phi'(0) \quad \text{where } m_w = D \left(\frac{\partial C}{\partial y} \right)_{y=0} = \frac{D}{\nu} (C_w - C_\infty) \phi'(0)$$

3. Method of Solving the Flow Equations

To find a computational solution for the current system, the Chebyshev spectra-collocation approach is used to the differential Eq. (16) to Eq. (18) with the boundary condition (19) and (20). Among its numerous advantages over other methods is that it has high accuracy, efficiency and ability to solve both nonlinear and linear ODEs/ PDEs systems of equations. Ehrenstein and Peyret [36] described the Chebyshev nth-order polynomial defined by $T_n(\zeta)$; $n \geq 0$ as

$$T_n(\zeta) = \cos(n \cos^{-1} \zeta); -1 \leq \eta \leq 1 \quad (21)$$

The recursive formula is written as $T_{n+1} = 2xT_n(x) - T_{n-1}(x)$; $n \geq 1$ the range of the flow $[0, \infty)$ is approximately taken as $[0, L]$ in order to introduce CSCM. The far domain of the boundary is L and the value of L defines the far stream convergence of the solution. Therefore, the range $[0, L]$ is converted to the range $[-1, 1]$ using the following algebraic definition

$$\zeta = \frac{2\eta}{L} - 1, \quad \zeta \in [-1, +1] \quad (22)$$

Let assume that $f(\eta)$, $\theta(\eta)$ and $\phi(\eta)$ are the unknown basis function $T_k(\zeta)$. to be approximated.

$$\left. \begin{aligned} f(\eta) &= \sum_{k=0}^N a_k T_k(\eta) \\ \theta(\eta) &= \sum_{k=0}^N b_k T_k(\eta) \\ \phi(\eta) &= \sum_{k=0}^N c_k T_k(\eta) \end{aligned} \right\} \quad (23)$$

Using the basis function in Eq. (20) where a_k , b_k and c_k are unknown coefficients to be obtained, in order to compute the residue, substituting (23) into the governing Eq. (16) to Eq. (18) the non-zero residue is determined. To minimizing error, residues are equated to zero at Nth collocation points. Chebyshev collocation points used is expressed according to Ehrenstein and Peyret [36].

$$\eta_j = \cos\left(\frac{\pi j}{N}\right), \quad j = 0, \dots, N. \quad (24)$$

This produces a $3N + 3$ set of algebraic equations along with the $3N + 3$ coefficient expansion a_k , b_k and c_k were determined. An iterative Newton's technique is employed on the resulting residues $N = 25$. The constants a_k , b_k and c_k are determined using MATHEMATICA software and substituted into Eq. (22) to obtain the computational results for the flow distributions.

4. Result and Discussion

The coupled nonlinear ordinary differential Eq. (16) to Eq. (18) subject to the boundary conditions (19) and (20) have been solved in this research by employing spectral collocation. In the numerical analysis a confirmation was made to observe the smoothness constraints within the boundary layer.

Figure 2 portrays the significance of the thermal relaxation parameter (α_1) on the velocity and temperature distributions. An increment in the value of α_1 is noticed to enhance the velocity and temperature profiles. Also, an enhancement in the hydrodynamic and thermal boundary layer is noticeable in Table 1 due to increase in α_1 . This outcome is correct because an increase in α_1 means that the particles of the material need more time to transfer heat to the neighbouring particles. It is worth noting that the Cattaneo-Christov model is transformed into the Fourier's law of heat conduction when $\alpha_1 = 0$.

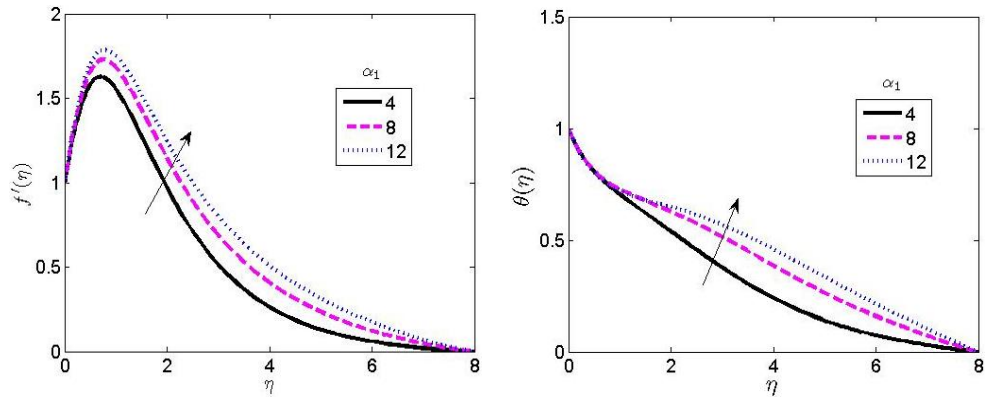


Fig. 2. Effect of thermal relaxation term on the velocity and temperature profiles

Table 1

Computational values of flow parameters on skin friction, Nusselt number and Sherwood number

λ_a	λ_b	M	Sc	Pr	R	Ec	α_1	Cr	τ	Do	So	C_f	Nh	Sh
0.0												0.0670	0.6935	0.8633
0.5												0.4084	0.6935	0.8633
1.0												0.7499	0.6935	0.8633
	0.0											0.2285	0.8299	0.3517
	0.5											0.5296	0.8299	0.3517
	1.0											0.8306	0.8299	0.3517
		1.0										1.7682	0.3582	0.3351
		2.0										1.4328	0.3582	0.3351
		3.0										0.6530	0.3582	0.3351
			0.22									1.8171	0.8101	0.6223
			0.38									1.6072	0.8101	0.7169
			1.0									1.4265	0.8101	0.8701
				0.71								1.4328	0.6935	0.4551
				3.0								0.9461	1.5919	0.4551
				7.0								0.7373	3.1771	0.4551
					0.0							1.4814	0.5530	0.8831
					0.5							1.7955	1.5543	0.8831
					1.0							2.0319	2.6617	0.8831
						0.2						1.8285	0.1793	0.6331
						0.5						2.2243	0.3350	0.6331
						0.7						2.6202	0.8494	0.6331
							0.5					1.8747	1.5473	0.7120
							1.0					2.0687	1.5582	0.7120
							1.5					2.1748	1.5830	0.7120
								0.0				1.2533	1.6935	1.0904
								0.5				0.8668	1.6935	1.5121
								1.0				0.6173	1.6935	1.6939
									1.0			2.4558	0.6920	0.4484
									2.0			3.4789	0.6920	1.7602
									3.0			4.5019	0.6920	3.0721
										2.0		1.9145	0.1430	0.8333
										3.0		2.3962	0.4075	0.8333
										4.0		2.8779	0.9580	0.8333
											2.0	1.6885	0.8299	0.1205
											3.0	1.9443	0.8299	0.2074
											4.0	2.2000	0.8299	0.5353

Figure 3 shows the impact of chemical reaction on the velocity and concentration profiles. An increase in the velocity and concentration profiles is noticeable for an increase in chemical reaction parameter. Physically, increasing chemical parameter means more chemical reactants are consumed and strength of homogenous reactions is enhanced which causes the concentration distribution to decrease. In Table 1, an increase in chemical reaction parameter is observed to decrease the skin friction coefficient but speed up the rate of mass transfer. No chemical change on the Nusselt number as chemical reaction parameter increases.

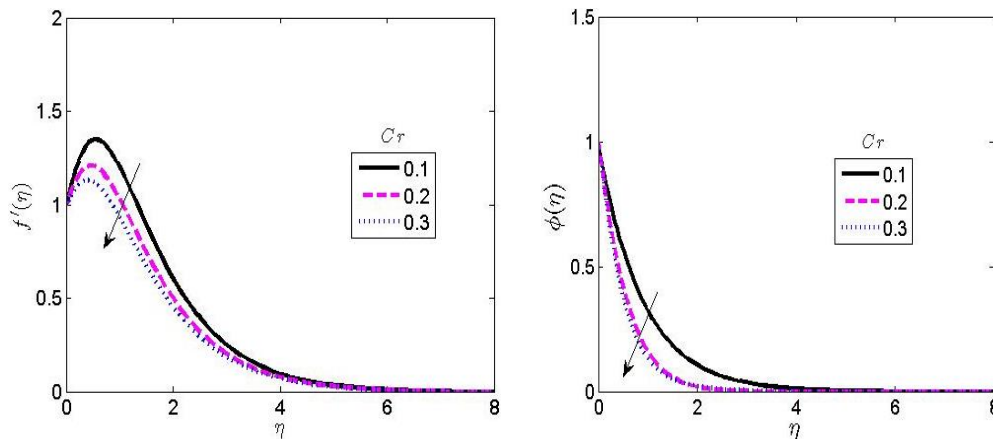


Fig. 3. Effect of chemical reaction parameter on the velocity and concentration profiles

Figure 4 illustrates the effects of Schmidt number (Sc) on the velocity and concentration profiles. A larger Schmidt number (Sc) is observed to declines the velocity and the concentration profiles. The Schmidt number (Sc) depicts the ratio of rate of viscous diffusion to the rate of molecular diffusion. Physically, or a fixed rate of molecular diffusion is to enhance the Schmidt number and the rate of viscous diffusion which leads to reduction in the fluid velocity.

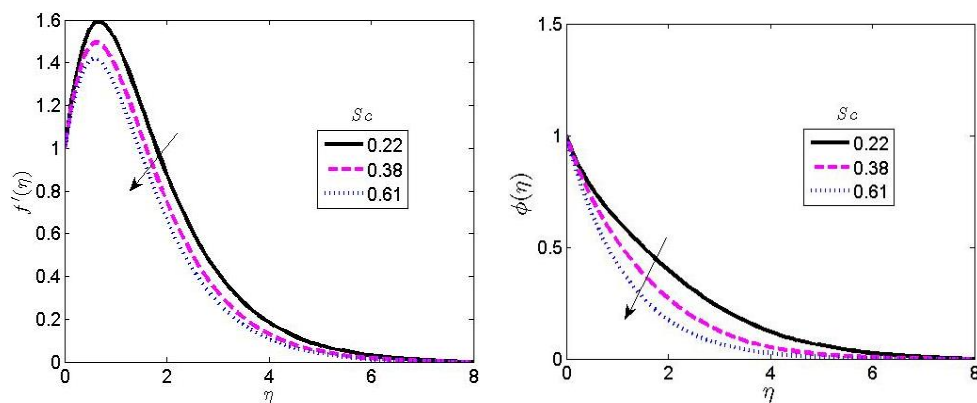


Fig. 4. Effect of Schmidt number on the velocity and concentration profiles

Figure 5 depicts the significance of Soret number (Sr) on the velocity and concentration profiles. The Soret parameter explains the temperature gradient when varying concentration. From Figure 5, an increment in the velocity and concentration is observed due to increase in Sr . Hence, a drastic increase in the hydrodynamic and thermal boundary layer is noticed on the Riga surface due to the presence of electromagnetic force.

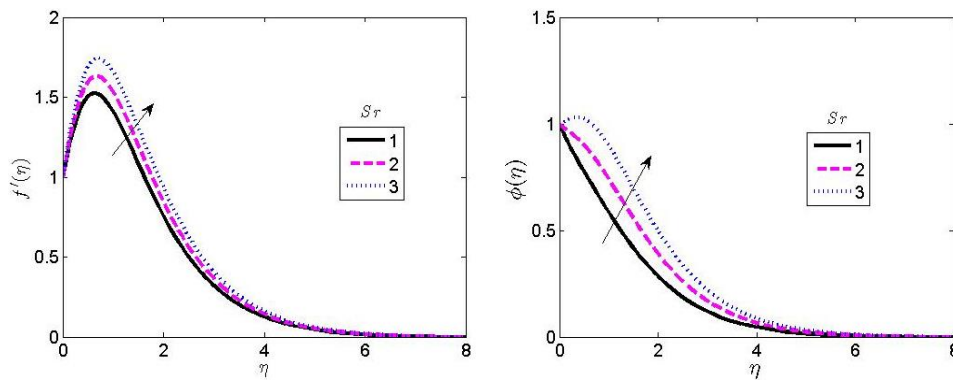


Fig. 5. Effect of Soret number on the velocity and concentration profiles

Figure 6 depicts the effects of Dufour parameter (Do) on the velocity and temperature profiles. The Dufour parameter means the significance of concentration gradients on temperature as illustrated in Figure 6. Physically, the Dufour parameter helps the fluid flow by increasing the thermal energy within the boundary layer. An increase in Table 1 (Do) is noticed to enhance the skin friction and the rate of heat transfer within the boundary layer.

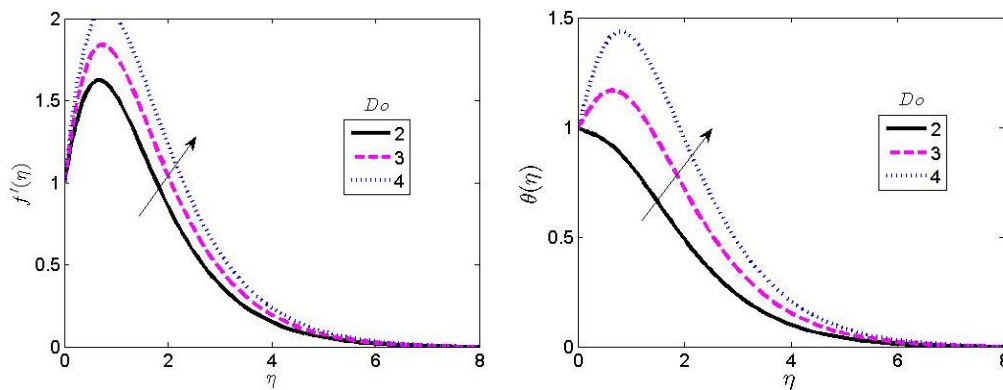


Fig. 6. Effect of Dufour number on the velocity and temperature profiles

Figure 7 depicts the impact of thermophoresis parameter on the velocity and concentration profiles. Physically, temperature gradient generates the thermophoresis between the hot and cold fluids. Hence, the fluid particles migrate from the hot region to the cold region during thermophoresis phenomenon within the boundary layer. An increase in thermophoresis parameter (τ) is observed to enhance the velocity and specie boundary layer.

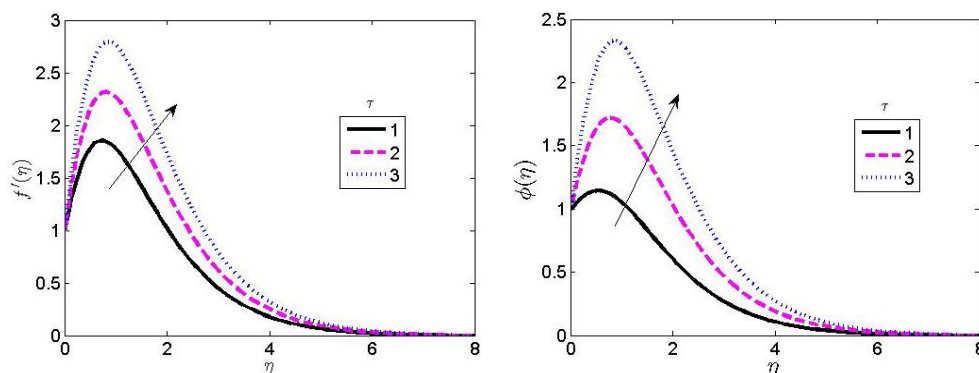


Fig. 7. Effect of thermophoresis parameter on the velocity and concentration profiles

Figure 8 depicts the Eckert number (Ec) on the velocity and temperature profiles. The outcomes in Figure 8 show that increase in Ec enhances the velocity and temperature distributions. Physically, the Eckert number is the relationship between the kinetic energy as well as the enthalpy in the flow. However kinetic energy is converted into internal energy due to work done in alternate to viscous fluid stresses. Therefore, greater dissipative heat leads to rise in fluid temperature and velocity.

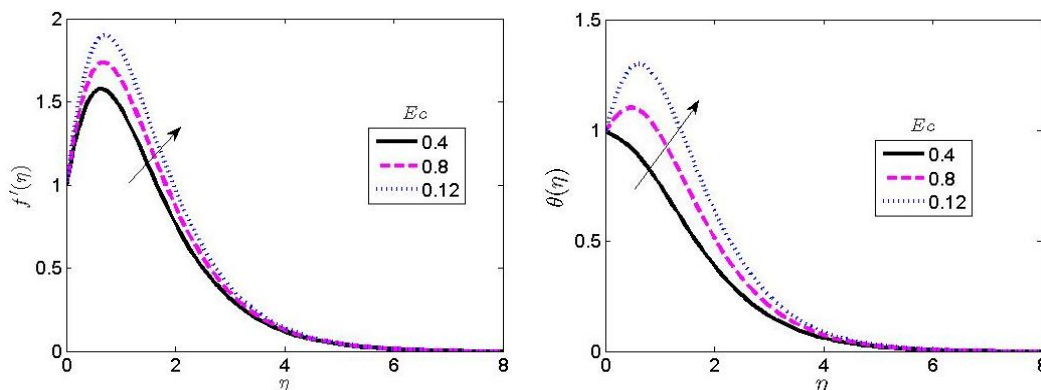


Fig. 8. Effect of Eckert number on the velocity and temperature profiles

Figure 9 shows the significance of Prandtl number (Pr) on the velocity and temperature profiles. In Figure 9, decrease in velocity and temperature is noticeable due to increase in Pr . The outcome is correct because fluids possessing higher Pr possess greater viscosities which lead to decrease in the temperature and velocity owing to this fact, the thickness of the hydrodynamic and thermal boundary layer decreases.

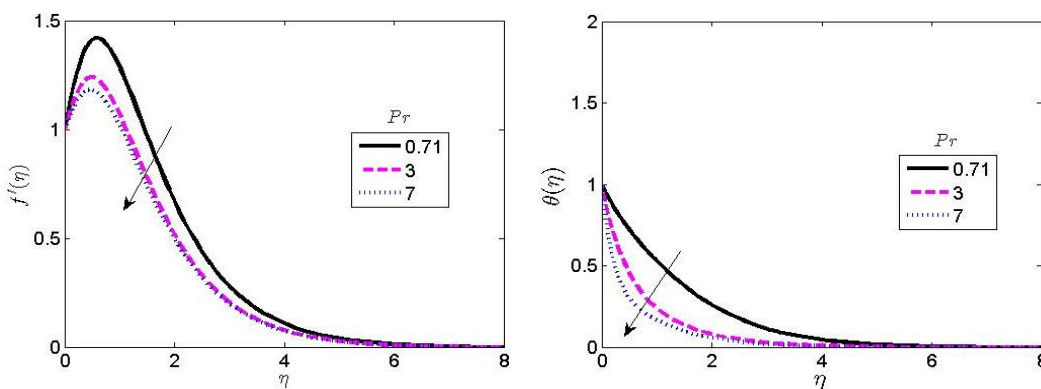


Fig. 9. Effect of Prandtl number on the velocity and temperature profiles

Figure 10 illustrates the effects of thermal radiation parameter (R) on the velocity and temperature profiles. Physically, thermal radiation parameter (R) brings enhancement to corrective flow [29]. An increment in thermal radiation parameter (R) leads to enhancement in velocity profile and the hydrodynamic layer. Physically, increase in thermal radiation parameter (R) leads to enhancement in the thermal condition of the fluid.

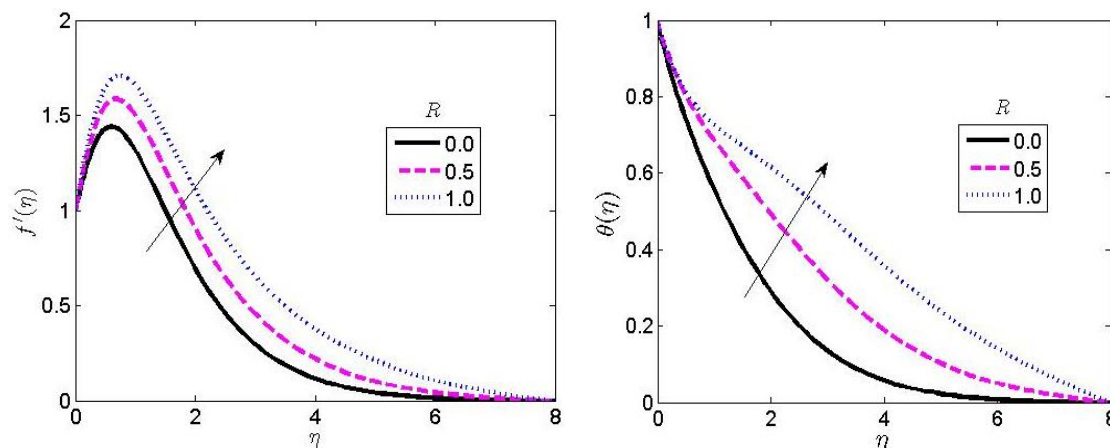


Fig. 10. Effect of thermal radiation on the velocity and temperature profiles

Figure 11 shows the effect of the nonlinear thermal Grashof number (λ_a) on the velocity profile. An increase in nonlinear thermal Grashof number (λ_a) is noticed to increase both velocity and the hydrodynamic boundary layer. The nonlinear thermal Grashof number (λ_a) creates a great buoyancy and viscous force within the boundary layer. Due to this force, more strength is imposed as nonlinear thermal Grashof number (λ_a) increases which leads to increase in fluid velocity.

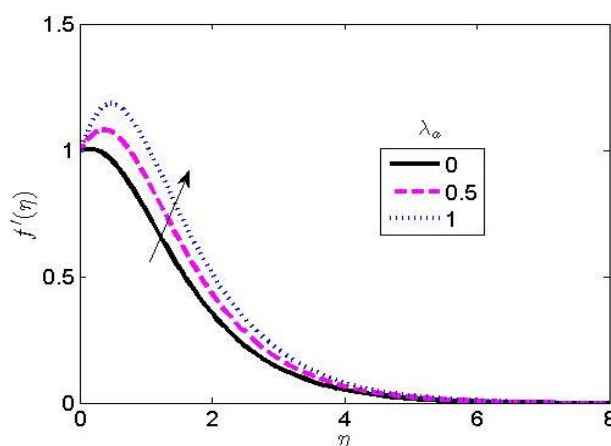


Fig. 11. Effect of nonlinear thermal Grashof number on the velocity profile

Figure 12 illustrates the effects of nonlinear mass Grashof number (λ_b). Increase in nonlinear mass Grashof number (λ_b) is observed to increase the fluid velocity. Increase in nonlinear mass Grashof number (λ_b) produces greater mass buoyancy which intensifies the velocity of the fluid. The impact of the modified Hartman number (M_q) in Table 1 shows decrease in the skin friction and the hydrodynamic boundary layer. Lorentz force is generated by the Riga plate parallel to the surface leads to a greater tension. It is this tension that drags the fluids within the hydrodynamic layer. Table 2 shows the comparison of the present result with that of Falodun and Omowaye [37].

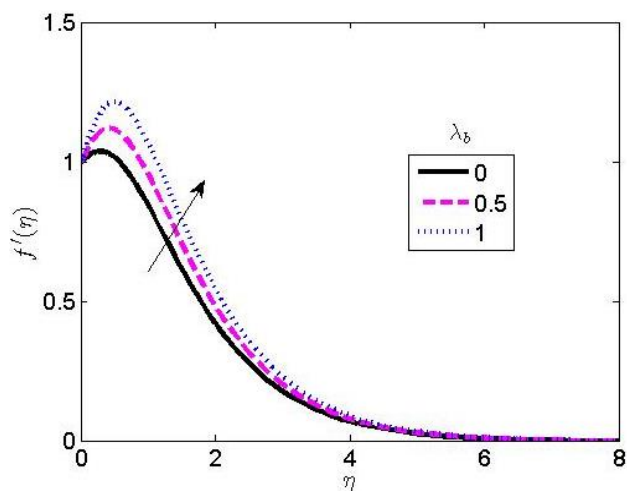


Fig. 12. Effect of nonlinear mass Grashof number on the velocity profile

Table 2

The comparison of the present result with the study of Falodun and Omowaye [37] when $\lambda_a = \lambda_b = M = \beta = \alpha_1 = Do = Sr = He = Ln = \tau = Nb = Nt = 0$

R	Present study			Falodun and Omowaye		
	$-f'(0)$	$-\theta'(0)$	$-\phi'(0)$	$-f'(0)$	$-\theta'(0)$	$-\phi'(0)$
0.5	0.33964676	0.61784821	1.78997668	0.33964678	0.61784823	1.78997670
1.0	0.34478444	0.62036542	1.90435546	0.34478446	0.62036544	1.90435548
1.5	0.34637964	0.62117872	2.02977907	0.34637963	0.62117871	2.02977905
2.0	0.35520227	0.62152515	2.15166865	0.35520227	0.62152513	2.15166863
3.0	0.37272860	0.62176435	2.37895292	0.37272858	0.62176433	2.37895290

Figure 13 shows the effect of Casson parameter (β) on the velocity profile. An increase in β is noticed to decrease the velocity profile. The Casson fluid is a yield exhibiting type of fluid which possesses a plastic dynamic viscosity which gives resistance to fluid flow.

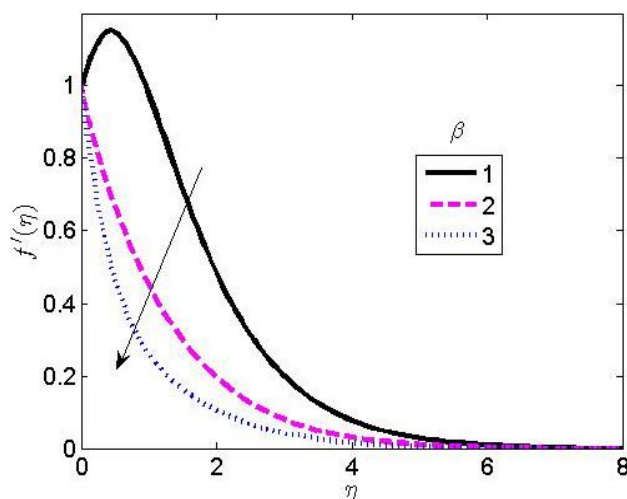


Fig. 13. Effect of Casson parameter on the velocity profile

Figure 14 shows the impact of the Brownian motion parameter (Nb) on the velocity and temperature profiles. The Brownian movement of the nanoparticles allows all particles to move in a constant motion. The movement of the nanofluids remains null over time. This shows that kinetic

energies possessed by molecular Brownian motions along with molecular vibrations sum up to obtain internal energy. Hence, increase in Brownian motion parameter (Nb) increases velocity and temperature distributions.

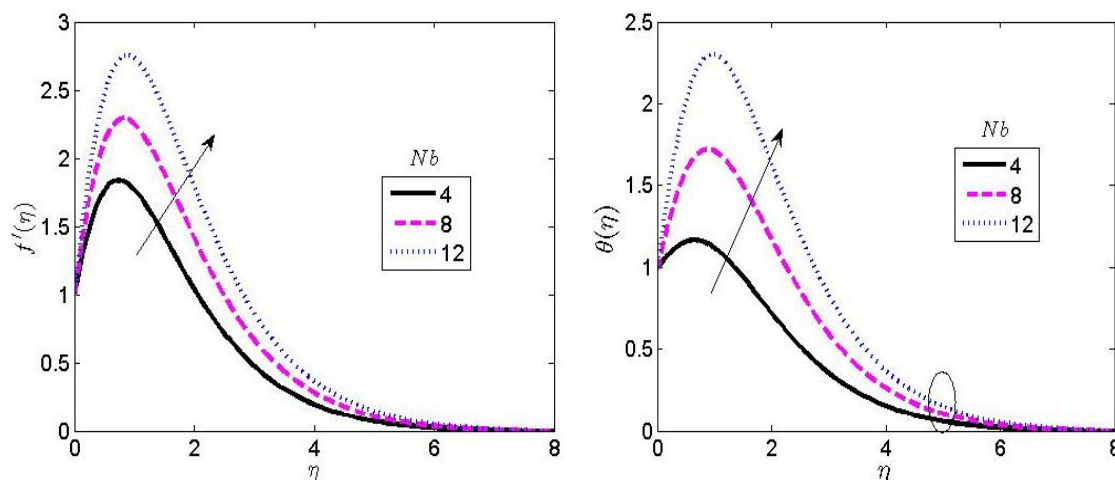


Fig. 14. Effect of Brownian motion parameter on the velocity and temperature profiles

In Figure 15, increase in the Riga surface term was found to elevate the fluid velocity.

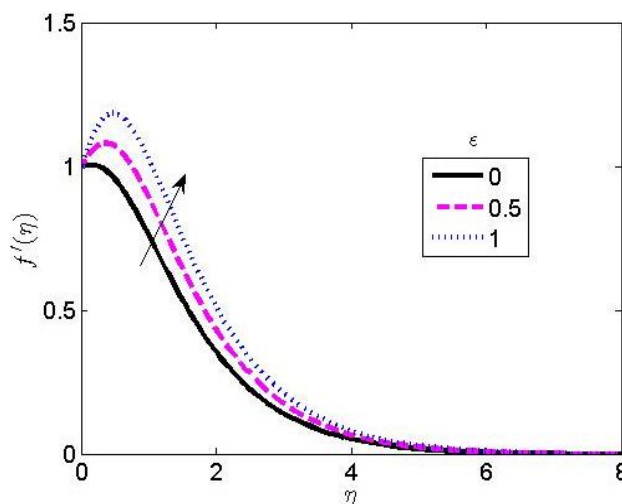


Fig. 15. Effect of Riga surface term on the velocity profile

5. Conclusion

This research explored the analysis of the model of double-diffusive free convective flow of chemically reacting fluids with nonlinear buoyancy force effects in a Riga plate. A parametric study was conducted to examine the significance of prominent parameters encountered in the problem. The radiative heat flux was described using the Rosseland approximation. In the research, a spectral based numerical approach is utilized to solve the coupled nonlinear ordinary differential equations. The following remarks are drawn from the research

- i. The modified Hartman number (M_q) produces Lorentz forces which brings tension to the parallel Riga plate to decrease the local skin friction;

- ii. An increase in the thermal radiation term (R) is noticed to enhance the velocity, temperature and the thermal condition of the fluid;
- iii. A larger Schmidt number (Sc) is observed to decline the fluid velocity and concentration;
- iv. A larger Prandtl number (Pr) is noticed to decrease the fluid velocity and temperature;
- v. A higher value of Eckert number (Ec) and Dufour parameter (Do) is observed to enhance the fluid velocity and temperature.

References

- [1] Gailitis, A. "On the possibility to reduce the hydrodynamic drag of a plate in an electrolyte." *Appl. Magnetohydrodynamics, Rep. Inst. Phys. Riga* 13 (1961): 143-146.
- [2] Iqbal, Z., Ehtsham Azhar, Zaffar Mehmood, and E. N. Maraj. "Melting heat transport of nanofluidic problem over a Riga plate with erratic thickness: Use of Keller Box scheme." *Results in Physics* 7 (2017): 3648-3658. <https://doi.org/10.1016/j.rinp.2017.09.047>
- [3] Rasool, Ghulam, and Ting Zhang. "Characteristics of chemical reaction and convective boundary conditions in Powell-Eyring nanofluid flow along a radiative Riga plate." *Heliyon* 5, no. 4 (2019): e01479. <https://doi.org/10.1016/j.heliyon.2019.e01479>
- [4] Loganathan, Parasuraman, and Krishnamurthy Deepa. "Electromagnetic and radiative Casson fluid flow over a permeable vertical Riga-plate." *Journal of Theoretical and Applied Mechanics* 57, no. 4 (2019): 987-998. <https://doi.org/10.15632/jtam-pl/112421>
- [5] Rehman, Khalil Ur, Qasem M. Al-Mdallal, and M. Y. Malik. "Symmetry analysis on thermally magnetized fluid flow regime with heat source/sink." *Case Studies in Thermal Engineering* 14 (2019): 100452. <https://doi.org/10.1016/j.csite.2019.100452>
- [6] Rehman, Khalil Ur, Iqra Shahzadi, M. Y. Malik, Qasem M. Al-Mdallal, and Mostafa Zahri. "On heat transfer in the presence of nano-sized particles suspended in a magnetized rotatory flow field." *Case Studies in Thermal Engineering* 14 (2019): 100457. <https://doi.org/10.1016/j.csite.2019.100457>
- [7] Rehman, Khalil Ur, M. Y. Malik, Mostafa Zahri, Qasem M. Al-Mdallal, Mohammed Jameel, and M. Imran Khan. "Finite element technique for the analysis of buoyantly convective multiply connected domain as a trapezium enclosure with heated circular obstacle." *Journal of Molecular Liquids* 286 (2019): 110892. <https://doi.org/10.1016/j.molliq.2019.110892>
- [8] Nasrin, Sonia, Rabindra Nath Mondal, and Md Mahmud Alam. "Impulsively started horizontal Riga plate embedded in unsteady Casson fluid flow with rotation." *Journal of Applied Mathematics and Physics* 8, no. 9 (2020): 1861-1876. <https://doi.org/10.4236/jamp.2020.89140>
- [9] Loganathan, Parasuraman, and Krishnamurthy Deepa. "Computational exploration of Casson fluid flow over a Riga-plate with variable chemical reaction and linear stratification." *Nonlinear Analysis: Modelling and Control* 25, no. 3 (2020): 443-460. <https://doi.org/10.15388/namc.2020.25.16659>
- [10] Rehman, Khalil Ur, Qasem M. Al-Mdallal, Iskander Tlili, and M. Y. Malik. "Impact of heated triangular ribs on hydrodynamic forces in a rectangular domain with heated elliptic cylinder: finite element analysis." *International Communications in Heat and Mass Transfer* 112 (2020): 104501. <https://doi.org/10.1016/j.icheatmasstransfer.2020.104501>
- [11] Rehman, Khalil Ur, Qasem M. Al-Mdallal, Aqeela Qaiser, M. Y. Malik, and M. N. Ahmed. "Finite element examination of hydrodynamic forces in grooved channel having two partially heated circular cylinders." *Case Studies in Thermal Engineering* 18 (2020): 100600. <https://doi.org/10.1016/j.csite.2020.100600>
- [12] Loganathan, K., Nazek Alessa, and Safak Kayikci. "Heat transfer analysis of 3-D viscoelastic nanofluid flow over a convectively heated porous Riga plate with Cattaneo-Christov double flux." *Frontiers in Physics* 9 (2021): 641645. <https://doi.org/10.3389/fphy.2021.641645>
- [13] Alam, Noor, Saykat Poddar, M. Enamul Karim, Mohammad Sanjeed Hasan, and Giulio Lorenzini. "Transient MHD Radiative Fluid Flow over an Inclined Porous Plate with Thermal and Mass Diffusion: An EFDM Numerical Approach." *Mathematical Modelling of Engineering Problems* 8, no. 5 (2021): 739-749. <https://doi.org/10.18280/mmep.080508>
- [14] Eswaramoorthi, S., Nazek Alessa, M. Sangeethavaanee, and Ngawang Namgyel. "Numerical and analytical investigation for Darcy-Forchheimer flow of a Williamson fluid over a Riga plate with double stratification and Cattaneo-Christov dual flux." *Advances in Mathematical Physics* 2021 (2021): 1-15. <https://doi.org/10.1155/2021/1867824>

- [15] Akaje, T. W., B. I. Olajuwon, and M. T. Raji. "Non-uniform heat source and melting heat effect on casson nanofluid flow over a Riga plate in the presence of nonlinear thermal radiation." *Journal of the Nigerian Association of Mathematical Physics* 64 (2022): 75-82.
- [16] Siegel, Robert, and John R. Howell. *Thermal radiation heat transfer*. McGraw-Hill, 1971.
- [17] Khan, Waqar Azeem, Masood Khan, Muhammad Irfan, and A. S. Alshomrani. "Impact of melting heat transfer and nonlinear radiative heat flux mechanisms for the generalized Burgers fluids." *Results in Physics* 7 (2017): 4025-4032. <https://doi.org/10.1016/j.rinp.2017.10.004>
- [18] Mondal, Munmun, Rajib Biswas, Kazi Shanchia, Mehedy Hasan, and Sarder F. Ahmmed. "Numerical investigation with stability convergence analysis of chemically hydromagnetic Casson nanofluid flow in the effects of thermophoresis and Brownian motion." *International Journal of Heat and Technology* 37, no. 1 (2019): 59-70. <https://doi.org/10.18280/ijht.370107>
- [19] Akinbo, B. Johnson, and Bakai I. Olajuwon. "Heat and mass transfer in magnetohydrodynamics (MHD) flow over a moving vertical plate with convective boundary condition in the presence of thermal radiation." *Sigma Journal of Engineering and Natural Sciences* 37, no. 3 (2019): 1031-1053.
- [20] Abdelmalek, Zahra, B. Mahanthesh, Md Faisal Md Basir, Maria Imtiaz, Joby Mackolil, Noor Saeed Khan, Hossam A. Nabwey, and I. Tlili. "Mixed radiated magneto Casson fluid flow with Arrhenius activation energy and Newtonian heating effects: flow and sensitivity analysis." *Alexandria Engineering Journal* 59, no. 5 (2020): 3991-4011. <https://doi.org/10.1016/j.aej.2020.07.006>
- [21] Tong, Zhao-Wei, Sami Ullah Khan, Hanumesh Vaidya, Rajashekhar Rajashekhar, Tian-Chuan Sun, M. Ijaz Khan, K. V. Prasad, Ronnason Chinram, and Ayman A. Aly. "Nonlinear thermal radiation and activation energy significances in slip flow of bioconvection of Oldroyd-B nanofluid with Cattaneo-Christov theories." *Case Studies in Thermal Engineering* 26 (2021): 101069. <https://doi.org/10.1016/j.csite.2021.101069>
- [22] Al-Khaled, Kamel, Sami Ullah Khan, and Ilyas Khan. "Chemically reactive bioconvection flow of tangent hyperbolic nanoliquid with gyrotactic microorganisms and nonlinear thermal radiation." *Heliyon* 6, no. 1 (2020): e03117. <https://doi.org/10.1016/j.heliyon.2019.e03117>
- [23] Irfan, Mohammad, M. Asif Farooq, Amaila Aslam, Asif Mushtaq, and Zahid Hussain Shamsi. "Magnetohydrodynamic time-dependent bio-nanofluid flow in a porous medium with variable thermophysical properties." *Mathematical Problems in Engineering* 2021 (2021): 1-16. <https://doi.org/10.1155/2021/6666863>
- [24] Lavanya, B., and A. Leela Ratnam. "The Effects of Thermal Radiation, Heat Generation, Viscous Dissipation and Chemical Reaction on MHD Micropolar Fluid Past a Stretching Surface in a Non-Darcian Porous Medium." *Global Journal of Engineering, Design and Technology* 3, no. 4 (2014): 28-40.
- [25] Pal, Dulal, and Sukanta Biswas. "Magnetohydrodynamic convective-radiative oscillatory flow of a chemically reactive micropolar fluid in a porous medium." *Propulsion and Power Research* 7, no. 2 (2018): 158-170. <https://doi.org/10.1016/j.jprr.2018.05.004>
- [26] Srinivasacharya, D., and P. Vijay Kumar. "Effect of thermal radiation on mixed convection of a nanofluid from an inclined wavy surface embedded in a non-Darcy porous medium with wall heat flux." *Propulsion and Power Research* 7, no. 2 (2018): 147-157. <https://doi.org/10.1016/j.jprr.2018.05.002>
- [27] Salawu, S. O., and M. S. Dada. "Radiative heat transfer of variable viscosity and thermal conductivity effects on inclined magnetic field with dissipation in a non-Darcy medium." *Journal of the Nigerian Mathematical Society* 35, no. 1 (2016): 93-106. <https://doi.org/10.1016/j.jnnms.2015.12.001>
- [28] Sarma, D., and K. K. Pandit. "Effects of Hall current, rotation and Soret effects on MHD free convection heat and mass transfer flow past an accelerated vertical plate through a porous medium." *Ain Shams Engineering Journal* 9, no. 4 (2018): 631-646. <https://doi.org/10.1016/j.asej.2016.03.005>
- [29] Babu, M. Jayachandra, N. Sandeep, and S. Saleem. "Free convective MHD Cattaneo-Christov flow over three different geometries with thermophoresis and Brownian motion." *Alexandria Engineering Journal* 56, no. 4 (2017): 659-669. <https://doi.org/10.1016/j.aej.2017.01.005>
- [30] Karimi, K., H. Roohani Ghehsareh, and K. Sadeghi. "An approximate solution for the MHD nano boundary-layer flows over stretching surfaces in a porous medium by rational Legendre collocation method." *Alexandria Engineering Journal* 56, no. 4 (2017): 687-694. <https://doi.org/10.1016/j.aej.2017.01.030>
- [31] Animasaun, I. L., and I. Pop. "Numerical exploration of a non-Newtonian Carreau fluid flow driven by catalytic surface reactions on an upper horizontal surface of a paraboloid of revolution, buoyancy and stretching at the free stream." *Alexandria Engineering Journal* 56, no. 4 (2017): 647-658. <https://doi.org/10.1016/j.aej.2017.07.005>
- [32] Mondal, Hiranmoy, Dulal Pal, Sewli Chatterjee, and Precious Sibanda. "Thermophoresis and Soret-Dufour on MHD mixed convection mass transfer over an inclined plate with non-uniform heat source/sink and chemical reaction." *Ain Shams Engineering Journal* 9, no. 4 (2018): 2111-2121. <https://doi.org/10.1016/j.asej.2016.10.015>

- [33] Gireesha, B. J., K. Ganesh Kumar, G. K. Ramesh, and B. C. Prasannakumara. "Nonlinear convective heat and mass transfer of Oldroyd-B nanofluid over a stretching sheet in the presence of uniform heat source/sink." *Results in Physics* 9 (2018): 1555-1563. <https://doi.org/10.1016/j.rinp.2018.04.006>
- [34] Akaje, Wasiu, and B. I. Olajuwon. "Impacts of Nonlinear thermal radiation on a stagnation point of an aligned MHD Casson nanofluid flow with Thompson and Troian slip boundary condition." *Journal of Advanced Research in Experimental Fluid Mechanics and Heat Transfer* 6, no. 1 (2021): 1-15.
- [35] Idowu, A. S., and B. O. Falodun. "Variable thermal conductivity and viscosity effects on non-Newtonian fluids flow through a vertical porous plate under Soret-Dufour influence." *Mathematics and Computers in Simulation* 177 (2020): 358-384. <https://doi.org/10.1016/j.matcom.2020.05.001>
- [36] Ehrenstein, U., and R. Peyret. "A Chebyshev collocation method for the Navier-Stokes equations with application to double-diffusive convection." *International Journal for Numerical Methods in Fluids* 9, no. 4 (1989): 427-452. <https://doi.org/10.1002/flid.1650090405>
- [37] Falodun, Bidemi Olumide, and Adeola John Omowaye. "Double-diffusive MHD convective flow of heat and mass transfer over a stretching sheet embedded in a thermally-stratified porous medium." *World Journal of Engineering* 16, no. 6 (2019): 712-724. <https://doi.org/10.1108/WJE-09-2018-0306>